

# Dynamics of Phospholipid Molecules in Micelles: Characterization with Fluorescence Correlation Spectroscopy and Time-Resolved Fluorescence Anisotropy

Mark A. Hink,<sup>†</sup> Arie van Hoek,<sup>‡</sup> and Antonie J. W. G. Visser<sup>\*,†</sup>

*MicroSpectroscopy Center, Department of Biomolecular Sciences, Laboratory for Biochemistry and Laboratory for Molecular Physics, Wageningen Agricultural University, Dreijenlaan 3, 6703 HA Wageningen, The Netherlands*

*Received July 27, 1998. In Final Form: November 9, 1998*

The dynamic properties of two BODIPY labeled phospholipid molecules in micellar systems have been studied with two different spectroscopic techniques, which provide complementary information (fluorescence correlation spectroscopy (FCS) and time-resolved fluorescence anisotropy (TRFA), respectively). One phospholipid had the fluorescent probe attached to the headgroup (abbreviated as head-labeled) and the other one had the probe at the acyl chain at the *sn*-2 position of the phospholipid (abbreviated as tail-labeled). From FCS experiments, the translational diffusion constant, aggregation number and hydrodynamic size of the micelles were determined. The micelles were larger in size than reported in the literature, which is due to the incorporation of the relatively large sized fluorescent probe. The FCS results were confirmed by the results of dynamic light scattering experiments on both empty micelles and micelles containing the fluorescent lipid probe. Both results showed that the probe has a very significant effect on the self-assembly behavior. The micelles loaded with the head-labeled phospholipid had a significantly larger radius compared to the micelles loaded with a tail-labeled probe. To obtain more insight into the intramicellar mobility and organization of the fluorescent lipid, TRFA experiments were performed. Analysis of the anisotropy decay showed that the lateral diffusion of the probe is the main, rapid contributing process in detergents such as Triton X-100, polyoxyethylene-9-lauryl ether (Thesit), cetyltrimethylammonium bromide (CTAB) and sodium dodecyl sulfate (SDS). However, digitonin and deoxycholate micelles had significantly different properties, which could be explained by more rigidly packed micelles. The calculated values for the wobbling motion, cone angle and order parameters indicated that the tail-labeled probe undergoes less restricted motion than the head-labeled probe.

## 1. Introduction

The plasma membrane has a crucial role in intracellular signal transduction processes. Membrane interactions involving proteins and lipid cofactors are continuously modulated enabling transmission of signals at the right moment and along the correct pathway. The physical structure of the lipid membranes strongly influences the dynamics of these processes. Therefore, experimental data on the spatial–temporal organization of the plasma membrane are required.

Because of their sensitivity, microspectroscopic techniques such as fluorescence correlation spectroscopy (FCS)<sup>1</sup> and time-resolved fluorescence anisotropy (TRFA)<sup>2</sup> provide quantitative information on molecular interactions and dynamic events. Prior to applying these techniques to relatively complex cellular membrane systems, one has to resort first to more simple model membranes. Therefore we have focused research to vesicles<sup>3</sup> and micelles as membrane mimetic systems. Although micelles do not mimic the exact biological bilayer, they have the

advantage that they form a simple experimental system. In this study it is demonstrated that FCS is a sensitive technique to determine the diffusion constant and size of single micelles loaded with amphiphilic fluorescent probes. TRFA provides complementary information on the intramicellar dynamics of the same micellar system as used in FCS. It turned out that the main depolarization mechanism is not rotation of the micelle as a whole, but internal restricted motion and lateral diffusion within the micelle.

## 2. Experimental Section

**Principle of FCS.** FCS is a technique developed in the early 1970s for studying single fluorescently marked molecules under equilibrium conditions.<sup>4–8</sup> In case of translational diffusion, the principle of FCS is as follows. A small open volume element of ca. 1.0 fL is created by a focused laser beam. In this confocal volume, fluorescent molecules will be excited and a burst of fluorescent photons is created. Owing to Brownian motion, molecules will enter or leave the excitation cavity, which results in changes of the detected fluorescence intensity. These intensity fluctuations provide information on diffusional properties of the fluorescent molecules, since small-sized molecules move more rapidly through the confocal volume element than large macromolecules. The diffusion constant for translational movement can be determined from the normalized autocorrelation function

\* To whom correspondence should be addressed. Telephone: +31-317-482862. Fax: +31-317-484801. E-mail: Ton.Visser@laser.bc.wau.nl.

<sup>†</sup> Laboratory for Biochemistry.

<sup>‡</sup> Laboratory for Molecular Physics.

(1) Thompson, N. L. In *Topics in Fluorescence Spectroscopy*; Lakowicz, J. R., Ed.; Plenum Press: New York, 1991; Vol. 1, p 337.

(2) Steiner, R. F. In *Topics in Fluorescence Spectroscopy*; Lakowicz, J. R., Ed.; Plenum Press: New York, 1991; Vol. 2, p 1.

(3) Hink, M.; Visser, A. J. W. G. In *Applied Fluorescence in Chemistry, Biology and Medicine*; Rettig, W., et al., Eds.; Springer-Verlag: Berlin; 1998, p 101.

(4) Elson, E. L.; Magde, D. *Biopolymers* **1974**, *13*, 1.

(5) Magde, D.; Elson, E. L.; Webb, W. W. *Biopolymers* **1974**, *13*, 29.

(6) Ehrenberg, M.; Rigler, R. *Chem. Phys.* **1974**, *4*, 390.

(7) Aragon, S. R.; Pecora, R. *Biopolymers* **1975**, *14*, 119.

(8) Magde, D.; Webb, W. W.; Elson, E. *Biopolymers* **1978**, *17*, 361.

$G(\tau)$ , which relates the fluorescence intensity,  $I$ , at a time  $t$  to that  $\tau$  seconds later:

$$G(\tau) = \frac{\langle I(t)I(t+\tau) \rangle}{\langle I \rangle^2} = \frac{\langle I \rangle^2 + \langle \delta I(t)\delta I(t+\tau) \rangle}{\langle I \rangle^2} \quad (1)$$

Here  $\delta I$  denotes the fluctuation of the fluorescence intensity around the mean value  $\langle I \rangle$ . The detected fluorescence intensity is dependent on the concentration and spectroscopic properties of the fluorescent probe and the detection efficiency of the experimental setup. Assuming a detection volume which is Gaussian shaped in three dimensions, the autocorrelation function can be written as

$$G(\tau) = 1 + \frac{(1 - F + F \cdot e^{-\lambda\tau})}{N_m \left(1 + \frac{4D_{\text{tran}}}{\omega_1^2 \tau}\right) \left(1 + \frac{4D_{\text{tran}}}{\omega_2^2 \tau}\right)^{1/2}} \quad (2)$$

where  $D_{\text{tran}}$  denotes the translational diffusion constant,  $N_m$  signifies the number of fluorescent particles in the detection volume and both  $\omega_1$  and  $\omega_2$  are constants corresponding to the radial and axial radii ( $e^{-2}$  point of the Gaussian beam) of the sample volume element. Equation 2 also contains a term  $F$ , describing the fraction of molecules in the triplet state and the characteristic triplet decay rate  $\lambda$ . The translational diffusion constant is related to the diffusion time  $\tau_{\text{diff}}$  via

$$D_{\text{tran}} = \frac{\omega_1^2}{4\tau_{\text{diff}}} \quad (3)$$

where  $\tau_{\text{diff}}$  is the time needed for the fluorescent particle to diffuse over a distance  $\omega_1$ . The square of the laser beam waist  $\omega_1$  can be obtained by calibration with a rhodamine 6G solution having a known diffusion constant of  $2.8 \times 10^{-10} \text{ m}^2 \text{ s}^{-1}$ .<sup>4</sup> The hydrodynamic radius of the fluorescent particle,  $r_h$ , is defined by eq 4 as

$$r_h = \frac{kT}{6\pi D_{\text{tran}} \eta} \quad (4)$$

where  $k$  is the Boltzmann constant,  $T$  the temperature, and  $\eta$  the viscosity. Assuming a spherical particle, the number of detergent molecules in the micelle,  $S$ , can be estimated by eq 5,

$$S = \frac{4\pi r_h^3 \rho N_a}{3m} \quad (5)$$

with  $\rho$  as the mean density of the micelle,  $N_a$  as Avogadro's number and  $m$  as the molecular mass of a single detergent molecule. It should be noted that eq 5 is a first-order approximation and that more elaborate equations should be applied for other shapes.

**Time-Resolved Fluorescence Anisotropy.** Time-resolved fluorescence anisotropy measurements yield detailed information on the motional freedom of the probe molecules in the micellar environment. By measuring the time-dependent parallel and perpendicular polarized emission components,  $I_{\parallel}(t)$  and  $I_{\perp}(t)$ , relative to the polarization of the exciting beam, the fluorescence anisotropy  $r(t)$  can be recovered:

$$r(t) = \frac{I_{\parallel}(t) - I_{\perp}(t)}{I_{\parallel}(t) + 2I_{\perp}(t)} \quad (6)$$

The fluorescence anisotropy decay was analyzed according to a general diffusion model, abbreviated  $r_{g3}$  (for details, see refs 9–11), in which the motion is described as diffusion in an anisotropic environment. Here it is assumed that the orientation of the labeled phospholipid is Gaussian distributed over a given angular width,  $\theta_g$ , around the micellar radius<sup>8</sup> (for this reason the model is referred to the modified  $r_{g3}$  model in the text). Although the  $r_{g3}$  model should be applied to analyze the anisotropy decay of cylindrically symmetrical probe molecules, it is unlikely to introduce a serious error using this model for the analysis of

the anisotropy decay of the (less symmetrical) fluorescent phospholipid probes. The fluorescence anisotropy decay curves of the fluorescent probes in micelles can be described by a product of three correlation functions (eq 7), corresponding to the internal motion of the probe, expressed by  $\theta_g$  and  $D_{\perp}$ , the probe lateral diffusion described by the lateral correlation time  $\phi_L$  and the overall rotation of the micelle with rotational correlation time  $\phi_R$ :<sup>8</sup>

$$r(t) = e^{-t/\phi_R} e^{-t/\phi_L} C(r_0, D_{\perp}, \theta_g, t) \quad (7)$$

where  $r_0$  is the fundamental anisotropy. The fluorescence anisotropy decay analysis requires therefore five parameters which are highly correlated. To simplify this analysis, some important assumptions have to be made. The micelles are expected to be globular and to behave as isotropic rotors. The overall rotational correlation time,  $\phi_R$ , can then be calculated from the FCS data using the Stokes–Einstein relationship (eq 8) and fixed in the analysis of the fluorescence anisotropy decay:

$$\phi_R = \frac{4\pi r_h^3 \eta}{3kT} \quad (8)$$

The fundamental anisotropy was obtained from the maximum entropy method (MEM) analysis of the fluorescence anisotropy decay<sup>12</sup> and was fixed as well. The lateral correlation time,  $\phi_L$ , is related to the lateral diffusion constant,  $D_{\perp}$ , and the position of the fluorescent group along the micellar normal,  $r_p$ , according to

$$\phi_L = \frac{r_p^2}{4D_{\perp}} \quad (9)$$

**Experimental Setup and Data Analysis.** FCS measurements were performed with a Zeiss-EVOTEC ConfoCor inverted confocal microscope. An air-cooled argon ion laser supplied two excitation wavelengths (488 and 514 nm) which was filtered by a  $515 \pm 15 \text{ nm}$  Omega interference filter and reflected by a Zeiss dichroic filter. The excitation light was focused by a water immersion objective (C-Apochromat 40 $\times$ , 1.2NA) into an eight-chambered coverglass (Nunc), containing the sample of investigation. The laser power was set with neutral density filters to less than 100  $\mu\text{W}$ . The fluorescent light was collected by the same objective, passed through the dichroic mirror and a 530–610 nm band-pass filter (Omega). The light passed through a motor-controlled pinhole (40  $\mu\text{m}$  diameter) in the image plane and is finally detected by an avalanche photodiode in single-photon counting mode, which signal was processed by a hardware correlator (ALV-5000, ALV, Langen, Germany). The sampling time of the correlator was between 200 ns and 3400 s using 288 (logarithmic spaced) time channels. The samples were measured over 20 s at 293 K.

The FCS experiments were analyzed with the FCS ACCESS software package developed by EVOTEC/Zeiss, Inc. (version 1.0.10), using the one-component fit model. This fit model determines the average number of fluorescent molecules in the detection volume as well as the characteristic diffusion time,  $\tau_{\text{diff}}$ , the triplet fraction,  $F$ , and the triplet lifetime,  $\lambda^{-1}$ . For analysis the curves were fitted with a fixed value for the structural parameter, which represents the ratio of  $\omega_2/\omega_1$  of the detection volume. This value was obtained from calibration with a rhodamine 6G solution.<sup>5</sup>

Time-resolved fluorescence anisotropy experiments were performed using the time-correlated single photon counting (TCSPC) technique.<sup>13</sup> For excitation a synchronously pumped dye laser with laser dye Coumarine 460 was used.<sup>14</sup> The pump

(9) Pap, E. H. W.; Ketelaars, M.; Borst, J. W.; van Hoek, A.; Visser, A. J. W. G. *Biophys. Chem.* **1996**, *58*, 255.

(10) Szabo, A. J. *Chem. Phys.* **1984**, *81*, 150.

(11) van der Meer, W. B.; Ameloot, M.; Hendrickx, H.; Schröder, H. *Biophys. J.* **1984**, *46*, 515.

(12) Brochon, J. C. *Methods Enzymol.* **1994**, *240*, 262.

(13) O'Connor, D. V.; Philips, D. *Time-Correlated Photon Counting*; Academic Press: London, 1984.

(14) van Hoek, A.; Visser, A. J. W. G. *Proc. SPIE*, **1992**, *1640*, 325.

laser is a 353 nm cw mode-locked Nd:YLF laser (Coherent model Antares 76-YLF with model 7600 mode locker). An electrooptic modulator setup in a dual-pass configuration was used to reduce the frequency of the light pulses from 76 MHz to 594.5 kHz. To prevent pile-up distortion, the energy of the excitation pulses was reduced by a variable density filters such that a maximum photon frequency of 30 kHz ( $\approx 5\%$  of 594 kHz) was obtained.<sup>15</sup> Excitation pulses ( $\lambda_{\text{ex}} = 512$  nm) were less than 4 ps full width at half-maximum with energies up to 2.6 nJ. Quartz cuvettes (1 cm path length in excitation, 1 cm<sup>3</sup> in volume) were placed in a thermostated holder (293 K). Fluorescence light was detected at an angle of 90° relative to the laser beam and passed through a combination of a OG 530 nm cutoff filter and a Balzers 550 band-pass filter ( $\Delta\lambda = 12$  nm). All measurements consisted of a number of sequences of measuring 10 s parallel ( $I_{\parallel}(t)$ ) and 10 s perpendicular ( $I_{\perp}(t)$ ) polarized emission. A total of 1024 channels were used per experimental decay with a time spacing of 50 ps per channel. The reference compound erythrosine B in nanopure water (with a known single lifetime of 80 ps) served as the reference compound to yield the dynamical instrumental response curve.<sup>16</sup>

The fluorescence anisotropy decay curves were analyzed with a global analysis program, obtained from Globals Unlimited Inc. (Urbana, IL)<sup>17</sup> and adapted using eq 7 as model function. The correlation times of the overall rotation of the micelles ( $\phi_R$ ), were calculated from the data obtained from FCS experiments, and the fundamental anisotropy ( $r_0$ ) was obtained from data analysis with the maximum entropy method (MEM).<sup>12</sup>

Dynamic light scattering (DLS) measurements were carried out by an experimental setup composed of a Lexel 150 mW multiline argon ion laser operating at 488 nm, a photomultiplier, and a personal computer containing an ALV-5000 correlator card. Samples consisted of 50 mM detergent in PBS with 0, 0.1, 0.5, or 5 mM of the fluorescent phospholipids. To exclude the fluorescence photons originating from the probe molecules, an Omega band-pass filter ( $475 \pm 15$  nm) was placed in front of the photomultiplier. Scattered intensities were recorded at a 90° scattering angle ( $\theta$ ) for 15 s per experiment, at 295 K. The diffusion constant  $D$  was obtained by fitting the experimental correlation curves,  $g^{(1)}(\tau)$ , according to

$$g^{(1)}(\tau) = e^{-Dq^2\tau} \quad \text{with} \quad q = (4\pi n_0/\lambda_{\text{ex}}) \sin(\theta/2) \quad (10)$$

with  $n_0$  the refractive index of the sample,  $\lambda_{\text{ex}}$  the excitation wavelength, and  $\theta$  the scattering angle.<sup>18</sup>

**Probes and Micelles.** The fluorescent probes used contain a charged phosphate group and hydrophobic (or lipophilic) acyl chains and therefore can easily be incorporated into micellar systems (Figure 1). The fluorescent probes were purchased from Molecular Probes, Inc (Eugene, OR) and were dissolved in stock in ethanol. BP-HPC (*C*<sub>5</sub>-HPC(2-(4,4-difluoro-5,7-diphenyl-4-bora-3a,4a-diaza-s-indacene-3-pentanoyl)-1-hexadecanoyl-*sn*-glycero-3-phosphocholine) consists of a phosphatidylcholine, with a fluorescent BODIPY group coupled to one of the fatty acyl chains. We will identify this as the tail probe. In BP-DHPE (*N*-(4,4-difluoro-5,7-diphenyl-4-bora-3a,4a-diaza-s-indacene-3-*propionyl*)-1,2-dihexadecanoyl-*sn*-glycero-3-phosphoethanolamine, triethylammonium salt) the BODIPY group was coupled to the phosphoethanolamine headgroup (identified as the head probe). The fluorescence quantum yields of these probes are close to one and are independent of pH and polarity of the local environment.<sup>19</sup>

The detergents were dissolved in PBS (8.8 g L<sup>-1</sup> NaCl, 0.2 g L<sup>-1</sup> KCl, 1.45 g L<sup>-1</sup> Na<sub>2</sub>HPO<sub>4</sub>·2H<sub>2</sub>O and 0.5 g L<sup>-1</sup> KH<sub>2</sub>PO<sub>4</sub> in

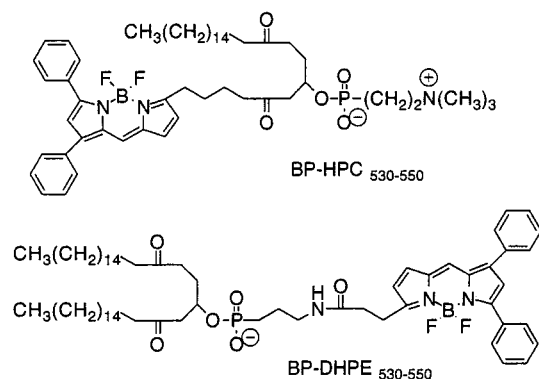


**Figure 1.** Molecular structures of the fluorescent phospholipids, BP-HPC and BP-DHPE.

Nanopure water): 5 mM CTAB (cetyltrimethylammonium bromide) (Serva), 5 mM digitonin (Sigma), 5 mM deoxycholate (Sigma), 10 mM SDS (sodium dodecyl sulfate) (BDH), 1 mM Triton X-100 (Merck), 1 mM Thesit (polyoxyethylene-9-lauryl ether) (Sigma), and 1 mM Tween 80 (polyoxyethylene sorbitan monooleate) (Merck). All solutions were set at pH 7.0 using 1 M HCl, except for digitonin which was dissolved at pH 8.3. Subsequently, the fluorescent probe was added (maximal 3 vol %) to a concentration of 10 nM in FCS experiments and 100 nM in fluorescence anisotropy experiments. Under these conditions, the probability of having more than one dye molecule per micelle is smaller than  $10^{-3}$ . The samples were bath-sonified for 1 min to guarantee that the probe is equally distributed among the available micelles and incubated for at least 10 min in the dark at 293 K before measurement.

DOPC vesicles (1-2-dioleoyl-*sn*-glycero-3-phosphocholine) (Avanti Polar Lipids, Inc.) were prepared from stocks in chloroform. The chloroform was evaporated with N<sub>2</sub> gas, to minimize oxidation. The lipids were dried in a vacuum desiccator for 20 min. 20  $\mu$ L of an ethanolic solution of fluorescent probe (either BP-HPC or BP-DHPE) and 980  $\mu$ L PBS buffer were added, and this mixture was bath-sonified for 1 min. The mixture was subsequently frozen with liquid N<sub>2</sub> and thawed with hot water (333 K). This cycle was repeated five times. The mixture was then transferred to a syringe and connected to a membrane filtration apparatus (Avestin). The mixture was pushed 35 times through a polycarbonate membrane with pores of 100 nm in diameter. This procedure resulted in single-sized vesicles.<sup>3</sup>

### 3. Results and Discussion

**Fluorescence Correlation Spectroscopy.** The autocorrelation curves, as obtained with FCS, were analyzed according to eq 2, using the one-component fit model, since analysis with two components did not result in improvement of the fits. A fraction of molecules with the typical diffusion time for free lipid probe was not found, indicating that all BODIPY probe molecules were taken up in the micelles. Figure 2 gives an example of the normalized autocorrelation curves of fluorescent Thesit and Triton X-100 micelles. The differences in the translational diffusion times between both detergents are clearly reflecting their micellar sizes. From the diffusion time the translational diffusion constant, hydrodynamic radius and aggregation number were calculated (see eqs 3–5). As can be seen from Table 1, the micellar radii are in the nanometer range and are in the same order as the radii of the fluorescent probes. Except for the cases of the nonionic detergents Triton X-100 and Thesit, the radii and aggregation numbers are larger than the literature values obtained with light scattering and sedimentation equilibrium experiments,<sup>20–24</sup> although the relative size

(15) Vos, K.; van Hoek, A.; Visser, A. J. W. G. *Eur. J. Biochem.* **1987**, *165*, 55.

(16) Visser, A. J. W. G.; van den Berg, P. A. W.; Visser, N. V.; van Hoek, A.; van den Burg, H. A.; Parsonage, D.; Claiborne, A. *J. Phys. Chem. B* **1998**, *102*, 10431.

(17) Beechem, J. M.; Gratton, E.; Ameloot, M.; Knutson, J. R.; Brand, L. In *Topics in Fluorescence Spectroscopy*; Lakowicz, J. R., Ed.; Plenum Press: New York, 1991; Vol 2, p 241.

(18) Pecora, R. *Dynamic Light Scattering*; Plenum Press: New York, 1985.

(19) Haugland, R. P. *Handbook of Fluorescent Probes and Research Chemicals*; Molecular Probes, Inc: 1996.

(20) Neugebauer, J. *A Guide to the Properties and Uses of Detergents in Biology and Biochemistry*; Calbiochem-Novabiochem International: 1994.

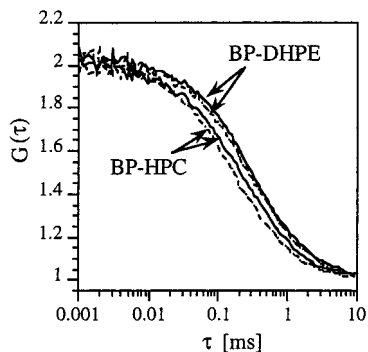


**Figure 2.** Normalized autocorrelation curves for Thesit (—) and Triton X-100 (---) micelles in PBS, loaded with BP-HPC or BP-DHPE. The following diffusion times were obtained:  $\tau_{\text{diff}}$  (Thesit, BP-HPC) =  $233 \pm 3 \mu\text{s}$ ;  $\tau_{\text{diff}}$  (Thesit, BP-DHPE) =  $323 \pm 4 \mu\text{s}$ ;  $\tau_{\text{diff}}$  (Triton, BP-HPC) =  $208 \pm 4 \mu\text{s}$ ;  $\tau_{\text{diff}}$  (Triton, BP-DHPE) =  $299 \pm 5 \mu\text{s}$ .

**Table 1. Translational Diffusion Constants, Calculated Rotational Correlation Times, Aggregation Numbers, and Hydrodynamic Radii of Several Detergents at pH 7.0 Loaded with 10 nM of BP-DHPE (first entry) or BP-HPC (second entry), As Determined with FCS<sup>a</sup>**

micelle	$D_{\text{tran}} \times 10^{11}$ ( $\text{m}^2 \text{s}^{-1}$ )	$\phi_R$ (ns)	aggregation no.	hydrodynamic radius (nm)
CTAB	$5.3 \pm 0.3$	69	$616 \pm 69$	$4.5 \pm 0.3$
	$6.6 \pm 0.3$	36	$319 \pm 41$	$3.7 \pm 0.2$
deoxycholate	$9.7 \pm 0.7$	11	$73 \pm 18$	$2.5 \pm 0.2$
	$11 \pm 1$	8	$50 \pm 13$	$2.2 \pm 0.2$
digitonin <sup>b</sup>	$3.4 \pm 0.3$	160	$541 \pm 65$	$7.1 \pm 0.4$
	$5.0 \pm 0.3$	81	$170 \pm 32$	$4.8 \pm 0.3$
SDS	$4.8 \pm 0.3$	94	$900 \pm 84$	$5.1 \pm 0.2$
	$6.5 \pm 0.4$	37	$357 \pm 51$	$3.7 \pm 0.2$
Thesit	$4.8 \pm 0.3$	90	$400 \pm 67$	$5.0 \pm 0.2$
	$6.9 \pm 0.4$	31	$136 \pm 22$	$3.1 \pm 0.2$
Triton X-100	$5.1 \pm 0.4$	77	$315 \pm 53$	$4.7 \pm 0.2$
	$7.7 \pm 0.4$	22	$92 \pm 19$	$3.5 \pm 0.3$
Tween 80	$5.0 \pm 0.4$	82	$160 \pm 41$	$4.8 \pm 0.4$
	$4.3 \pm 0.3$	128	$250 \pm 68$	$5.6 \pm 0.5$

<sup>a</sup> The overall micellar correlation time,  $\phi_R$ , was calculated from FCS experiments. The micelles are assumed to have a spherical shape with a density of  $1.05 \text{ g cm}^{-3}$  in a solution with a viscosity of  $1 \times 10^{-3} \text{ Pa s}$ . Standard errors are based on multiple measurements ( $n = 15$ ). <sup>b</sup> Except the digitonin solution which had pH 8.3.

differences between the micelles were in agreement with literature. It should be noted that in our calculations the aggregates are assumed to have a spherical shape, which may be not accurate for all detergents. On the other hand, our aim was to compare the overall and internal dynamics of a series of micelles, and the spherical shape as a first-order parameter approximation is therefore justified. It should also be emphasized that FCS selectively monitors the micelles which are loaded with a fluorescent phospholipid.

Additional dynamic light scattering experiments (DLS) were performed to check if the differences were caused by the incorporation of the relatively large probe molecules. As can be seen in Table 2, the diffusion constants for unlabeled micelles, obtained with DLS, were comparable to the calculated literature values.<sup>20–25</sup> Addition of fluorescent probe molecules to the micelles, in a ratio of

**Table 2. Diffusion Constants ( $\times 10^{11} \text{ m}^2 \text{ s}^{-1}$ ) from Micellar Systems with or without BP-DHPE (First Entry) or BP-HPC (Second Entry) as Monitored with Dynamic Light Scattering and Fluorescence Correlation Spectroscopy<sup>a</sup>**

	without fluorescent probe		with fluorescent probe	
	lit.	DLS	DLS	FCS
CTAB	8.0	$7.3 \pm 0.4$	$5.2 \pm 0.5$	$5.3 \pm 0.3$
deoxycholate	21		$6.4 \pm 0.4$	$6.6 \pm 0.3$
			$9.7 \pm 0.7$	$11 \pm 1$
digitonin	4.2	$4.3 \pm 0.2$	$3.8 \pm 0.5$	$3.4 \pm 0.3$
			$5.6 \pm 0.8$	$5.0 \pm 0.3$
SDS	11	$10.2 \pm 0.4$	$4.9 \pm 0.3$	$4.8 \pm 0.3$
			$7.0 \pm 0.5$	$6.5 \pm 0.4$
Thesit	4.0	$4.5 \pm 0.3$	$4.6 \pm 0.3$	$4.8 \pm 0.3$
			$5.8 \pm 0.6$	$6.9 \pm 0.4$
Triton X-100	4.8	$4.4 \pm 0.3$	$5.0 \pm 0.6$	$5.1 \pm 0.4$
			$5.8 \pm 0.8$	$7.7 \pm 0.4$
Tween 80	4.2	$4.5 \pm 0.3$	$5.5 \pm 0.5$	$5.0 \pm 0.4$
			$3.9 \pm 0.4$	$4.3 \pm 0.3$

<sup>a</sup> Literature values were calculated from available micellar radii or aggregation numbers assuming spherical shaped micelles with a density of  $1.05 \text{ g cm}^{-3}$ . Standard errors are based on multiple measurements ( $n = 15$ ).

approximately one fluorophore per micelle, resulted in a significant decrease of the diffusion constant. The diffusion constants became similar to the values obtained with FCS. These observations strongly suggest that the incorporation of a relatively large fluorescent phospholipid perturbs the micellar structure: extra detergent molecules are required to “solubilize” the fluorescent group, resulting in an increase of the hydrodynamic radius and aggregation number. The main conclusion from both FCS and DLS experiments is therefore that the probe has a significant effect on the self-assembly of the surfactant molecules resulting in distinctly larger particles.

The autocorrelation curves in Figure 2 show that the labeling-position of the BODIPY group in the phospholipid molecule strongly affects the micellar characteristics: Thesit and Triton X-100 micelles loaded with the tail-labeled probe, BP-HPC, moved faster through the detection volume than the micelles loaded with the head-labeled BP-DHPE, as can also be seen from the diffusion constants presented in Table 1. Except for Tween 80, the translational diffusion constants of BP-DHPE-loaded micelles are roughly 30% smaller than those of the BP-HPC-loaded aggregates. These differences are most likely caused by the different locations of the fluorescent groups: The BODIPY group of BP-HPC is coupled to one of the hydrophobic acyl chains of the phospholipid and will therefore be located in the micellar core between the hydrophobic chains of the detergent molecules. In contrast, the large fluorescent headgroup of BP-DHPE is expected to be positioned near the micellar interface, because the negatively charged phosphate group will prevent the fluorescent moiety to get solubilized in the hydrophobic micellar core. BP-DHPE will therefore require some more detergent molecules to “solubilize” the BODIPY group, which is reflected in the larger aggregation number compared to BP-HPC-loaded micelles. The hydrodynamic radii of the BP-DHPE-loaded micelles are 1.1–1.6 times larger than those of the BP-HPC-loaded micelles.

Both apparent anomalies, namely the larger micellar sizes of phospholipid-filled micelles as compared to non-filled ones and the size differences connected with the selected fluorescent probe lipid, are consequences of the fact that the dimensions of the fluorescent phospholipids are of nonnegligible magnitude as compared to micellar

(21) Maiti, N. C.; Mazumdar, S.; Periasamy, N. *J. Phys. Chem.* **1995**, *99*, 9, 10708.

(22) Fendler, J. H. *Membrane Mimetic Chemistry*. Wiley-Interscience: New York, 1982.

(23) Robson, R. J.; Dennis, E. A. *J. Phys. Chem.* **1977**, *81*, 1075.

(24) Quitevis, E. L.; Marcus, A. H.; Fayer, M. D. *J. Phys. Chem.* **1993**, *97*, 5762.

(25) Zana, R.; Levy, H.; Danino, D.; Talmon, Y.; Kwetkat, K. *Langmuir* **1997**, *13*, 402.

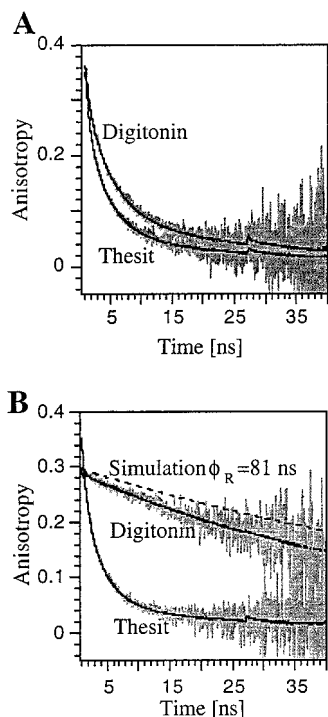


**Figure 3.** Experimental fluorescence anisotropy decay curves of digitonin and Thesit micelles loaded with BP-DHPE (A) or BP-HPC (B). The solid, smooth curve corresponds to the optimal fit with the modified  $r_{g3}$  model assuming a Gaussian orientation distribution. Also included in panel B is a simulated anisotropy decay curve (---) assuming only micellar rotation ( $\phi_R = 81$  ns) for contribution to the anisotropy decay.

dimensions. To prove this point we have carried out size determinations of single unilamellar vesicles (SUVs) of DOPC, which are much larger than the micelles used in this study and which are separately loaded with both fluorescent lipid probes. The hydrodynamic radii of BP-HPC-loaded vesicles ( $36 \pm 10$  nm) and BP-DHPE-loaded vesicles ( $38 \pm 12$  nm) were exactly the same within experimental error.

**Time-Resolved Fluorescence and Fluorescence Anisotropy.** Time-resolved fluorescence experiments revealed that the fluorescence intensity decayed in a nonexponential fashion. When the fluorescence decay was analyzed in distributed fluorescence lifetimes, using the MEM approach, four peaks were observed at 0.054, 0.35, 2.5, and 5.6 ns. The lifetime distribution patterns for both types of fluorescent probe were similar and independent of the type of detergent (data not shown). This indicates that the depopulation mechanism of the excited state is independent of the local environment. These observations are supported by experiments,<sup>19</sup> which showed that the fluorescence quantum yield of BODIPY fluorophores is relatively insensitive to the environment. The fluorescence lifetime distributions were also insensitive to a 10-fold increase or decrease of the dye concentration. Hence the effect of excitation energy transfer between fluorescent probe molecules can be neglected, as was expected at the probe concentrations used.

In Figure 3 the fluorescence anisotropy decay curves for digitonin and Thesit micelles are presented. Both micelles were loaded with either BP-HPC or BP-DHPE. The smooth curves through the data points represent the optimized fits according to the modified  $r_{g3}$  model (eq 7) with the assumption that the orientation distribution of the fluorescent probe is Gaussian shaped around the micellar radius with angular width  $\theta_g$ . It can be seen that the decay curve for the Thesit micelles loaded with BP-

DHPE (panel A) is similar to the curve for BP-HPC-loaded Thesit micelles (panel B). However, the anisotropy decay of BP-DHPE-loaded digitonin is considerably slower than for Thesit micelles and even much slower for digitonin micelles loaded with BP-HPC. The dotted line in panel B represents a simulated curve for the case that only the rotational motion of the whole micelle ( $\phi_R = 81$  ns) contributes to the anisotropy decay. The experimental data for BP-HPC loaded digitonin follows this simulated curve quite close, indicating that the contribution of other depolarization processes is small. As will be discussed later, the molecular structure of the detergent molecules seems to have a strong effect on the motional freedom of the probes in the micelles.

In Table 3 all the recovered anisotropy parameters, as determined with the modified  $r_{g3}$  fit-model, are presented. The fundamental anisotropy was determined with MEM analysis and varied between 0.30 and 0.37, which is close to the maximum possible value of 0.4 when the absorption and emission moments are parallel. Analysis of the anisotropy decay data revealed that in most cases the contribution of the intramicellar, lateral diffusion of the probe was roughly five times larger than the contribution of the micellar rotation (data not shown). Hence, the uncertainty in the rotational correlation time  $\phi_R$  is large. Therefore these values were calculated from FCS experiments (eq 7) and fixed in the analysis. However, for digitonin and deoxycholate the contribution of the lateral diffusion was found to be small ( $\sim 8\%$ ). Analysis according to the modified  $r_{g3}$  fit-model showed that the uncertainty of the lateral correlation times in both detergents was large and even negative values showed up in the error of the analysis (Table 3). The lateral diffusion constants are therefore small, indicating a severe restriction of the lateral movement. Since in these micelles the lateral and rotational diffusion processes occur in the same order of time, the modified  $r_{g3}$  model should not be applied to fit the experimental data. The restriction of the lateral motion of deoxycholate and digitonin can be explained by their molecular structures. Both detergent molecules are flat and rigid, consisting of several fused cyclic carbon rings. In contrast to the other detergents, deoxycholate and digitonin seems to be able to form rigid, cage-like structures in the micellar core which tightly accommodates the fluorophore. In this way the lateral mobility of the fluorescent probe is strongly limited.

The intramicellar lateral diffusion constants were calculated using eq 9 with the assumption that the fluorescent group of BP-HPC is located 1 nm under the micellar surface and at the micellar interface for BP-DHPE. The lateral diffusion constants for the head-labeled phospholipid are in the order of  $10^{-10}$  m<sup>2</sup> s<sup>-1</sup>, and except for Tween 80, almost five times lower than for the tail-labeled probe. The intramicellar diffusion is in the same order as the lateral diffusion of BP-HPC in vesicles<sup>3</sup> but much faster than rhodamine-labeled dipalmitoylphosphatidylethanolamine (DPPE-Rh) and *N*-4-nitrobenzo-2-oxa-1,3-diazolelaurate (NBD-C12) in black lipid membranes (BLM).<sup>26,27</sup> In BLM's the diffusion constants were on the order of  $10^{-11}$  m<sup>2</sup> s<sup>-1</sup> while whole vesicles have a  $D_{\text{tran}} \approx 10^{-12}$  m<sup>2</sup> s<sup>-1</sup>. These observations can be explained by differences in packing, which is less tight in the curved micelles than in the lipid bilayers. In models for lateral diffusion, molecules move by exchanging positions or by migrating through gaps or interstitial sites in the membrane.<sup>28,29</sup> On the basis of these jump-models, the lateral diffusion will be faster when the surfactant molecules are more loosely packed.

(26) Fahey, P. F.; Koppel, D. E.; Barak, L. S.; Wolf, D. E.; Elson, E. L.; Webb, W. W. *Science* **1977**, *195*, 305.

(27) Fahey, P. F.; Webb, W. W. *Biochemistry* **1978**, *17*, 3046.

**Table 3. Anisotropy Decay Parameters (See text) Obtained from the Global Analysis of Micelles Loaded with 100 nM BP-DHPE (First Entry) or BP-HPC (Second Entry)<sup>a</sup>**

micelle	$\phi_L$ (ns)	$D_L$ (m <sup>2</sup> s <sup>-1</sup> )	$D_{\perp}$ ( $\mu$ s <sup>-1</sup> )	$\theta_g$ (rad)	$r_0$	$P_2$	$P_4$	$\chi^2$
CTAB	20 (15–31)	$2.5 \times 10^{-10}$	53.6 (51.8–56.6)	0.59 (0.58–0.65)	0.33	0.60	0.18	1.27
	17 (12–28)	$1.1 \times 10^{-10}$	63.9 (61.8–66.7)	0.66 (0.60–0.73)	0.33	0.53	0.12	1.25
deoxycholate	21 (13–73)	$7.4 \times 10^{-11}$	31.2 (27.0–33.7)	0.74 (0.54–0.83)	0.36	0.46	0.07	1.25
	29 (–18–85)	$1.2 \times 10^{-11}$	28.9 (23.4–32.8)	0.73 (0.49–0.83)	0.37	0.46	0.07	1.25
digitonin	79 (69–105)	$1.6 \times 10^{-10}$	30.1 (1.0–384)	0.99 (0.94–0.99)	0.31	0.88	0.84	1.23
	154 (–80–230)	$4.4 \times 10^{-11}$	32.0 (3.0–500)	0.99 (0.97–0.99)	0.30	0.99	0.95	1.39
SDS	14 (8–27)	$4.6 \times 10^{-10}$	80.7 (78.5–85.6)	0.71 (0.63–0.81)	0.32	0.48	0.09	1.39
	14 (9–21)	$4.9 \times 10^{-11}$	89.4 (86.3–94.1)	0.79 (0.72–0.83)	0.32	0.40	0.05	1.35
Thesit	25 (14–37)	$2.2 \times 10^{-10}$	50.7 (48.6–54.2)	0.57 (0.52–0.65)	0.34	0.62	0.20	1.30
	22 (15–27)	$5.1 \times 10^{-11}$	57.3 (56.6–59.2)	0.65 (0.59–0.72)	0.34	0.55	0.13	1.25
Triton X-100	32 (22–47)	$1.7 \times 10^{-10}$	21.5 (20.6–23.6)	0.42 (0.35–0.51)	0.36	0.77	0.43	1.27
	19 (15–32)	$8.2 \times 10^{-11}$	21.4 (21.5–23.1)	0.43 (0.37–0.56)	0.36	0.76	0.39	1.17
Tween 80	21 (17–32)	$2.7 \times 10^{-10}$	31.6 (30.0–34.1)	0.49 (0.43–0.56)	0.34	0.70	0.30	1.32
	21 (15–33)	$2.5 \times 10^{-10}$	32.9 (32.2–35.0)	0.53 (0.46–0.61)	0.35	0.66	0.26	1.27

<sup>a</sup> The fundamental anisotropy,  $r_0$ , was obtained from MEM analysis. The lateral diffusion constant  $D_L$  was calculated according to eq 10, assuming the positions of the fluorescent groups for BP-DHPE and BP-HPC at 0 and 1 nm, respectively, under the micellar surface. The numbers between parenthesis correspond to the errors as determined from a rigorous error analysis at a 67% confidence level, as described elsewhere.<sup>9</sup>  $\chi^2$  indicates the quality of the fit.

The angular range ( $\theta_g$ ) over which the probes are moving varies between 0.4 and 0.8 rad with relatively high uncertainties. Since the errors of  $\theta_g$  at a 67% confidence level are within the error of the experiment, no differences are seen between the two different probe in micelles of deoxycholate, Triton X-100 and Tween 80. However, the tail-labeled probes in CTAB, digitonin, SDS, and Thesit micelles possesses a significantly larger angle (around the micellar radius) than the head-labeled probe. Although the fluorescent BODIPY group is large, containing several aromatic rings, it seems that in the micellar core the probe can move more freely than near the micellar surface. This agrees with the thermodynamic theory<sup>28–30</sup> and spectroscopic experiments<sup>31,32</sup> which showed that the core of micelles and the interior of lipid bilayers behave as an organic fluid.

The local order around the phospholipid probe is described by the second-rank and fourth-rank order parameters ( $P_2$ ) and ( $P_4$ ).<sup>8–10</sup> These values are very high for the digitonin micelles, indicating a highly ordered local environment as was expected on the basis of the detergent structure discussed above. Although similar results were expected for deoxycholate, the local order seems to be lower than in the other micelles. Comparison of the local order between the two fluorescent probes showed that the order around the head-labeled probe is higher, again consistent with the model which describes the micellar core as a liquid hydrocarbon experiencing a relatively lower order than the interfacial environment around the ionic head-group probe.

The wobbling diffusion constants  $D_{\perp}$ , representing the internal rotation of the probe, are listed in Table 3. The wobbling motion of the probes in the negatively charged SDS micelles is significantly faster than in the positively charged CTAB micelles. It seems that the electrostatic repulsion between the negatively charged phosphate group of the fluorescent probe and the SDS detergent molecules will increase the distance between the headgroups, thereby creating space for less restricted wobbling motion. The wobbling motion in the nonionic micelles is relatively slow compared to the two charged detergents. Quitevis et al.

found similar results for the charged M540 probe in micelles made from various detergents.<sup>24</sup> The latter authors proposed that in nonionic micelles the charged headgroup of the fluorescent probe protrudes out of the micelle into the water region. Due to stronger interactions between the water molecules and the phosphate group, the fluorescent probe will be more motionally restricted. Large-sized molecules are expected to be packed more densely, resulting in a lower wobbling rate. However, in our experiments, no correlation between the micellar radius and the wobbling constant was found. The wobbling motion of the tail-labeled BP-HPC is slightly faster than that for BP-DHPE. Probably the internal motion in the micellar core is less restricted than near the micellar interface. The rates are similar to the ones found for BP-HPC and diphenylhexatriene-PC (DPH-PC) in DOPC vesicles<sup>3,9</sup> but are almost 10 times smaller than the wobbling rates of the single-chained M540 and octadecyl Rhodamine B in micelles<sup>24</sup> or porphyrins in micelles.<sup>21</sup>

### Concluding Remarks

A combination of fluorescence correlation spectroscopy and time-resolved fluorescence anisotropy provides detailed information of the dynamics of phospholipid probes in micelles, although the relatively large size of the fluorescent probes caused a disturbance of the relatively small micellar structures as has been confirmed by dynamic light scattering experiments. The relative size differences of the micelles and the motional properties of the fluorescent probes correspond well with literature values. Future studies will focus on the dynamical properties of the fluorescent probes in more complicated lipid systems, which mimic more closely the cell membrane.

**Acknowledgment.** We thank Eward Pap for his help in the fluorescence anisotropy decay analysis and Remko Fokkink and Martien Cohen Stuart for generous access to the dynamic light scattering experiments. Peter Bremer and Reinhard Janka from Carl Zeiss, Inc., are gratefully acknowledged for technical and financial support. This research was supported by an investment grant from The Netherlands Organization for Scientific Research (NWO) and by a grant from the Earth and Life Sciences Foundation of NWO.

(28) Houslay, M. D.; Stanley, K. K. *Dynamics of Biological membranes*; Wiley: New York, 1982; Vol. 91, p 39.

(29) Silver, B. L. *The physical chemistry of membranes*; Solomon Press: New York, 1985; p 75.

(30) Benjamin, L. *J. Phys. Chem.* **1966**, *70*, 3790.

(31) Waggoner, A. S.; Griffith, O. H.; Christensen, C. P. *Proc. Natl. Acad. Sci. U.S.A.* **1967**, *57*, 1198.

(32) Rosenholm, J. B.; Drakenberg, T.; Lindman, B. *J. Colloid Interface Sci.* **1978**, *63*, 538.